NRIAG JOURNAL OF ASTRONOMY AND GEOPHYSICS
2019, VOL. 8, NO. 1, 231–241
https://doi.org/10.1080/20909977.2019.1689629



# Application of high-resolution gravity data for litho-structural and depth characterisation around Igabi area, Northwestern Nigeria

C. C. Okpoli and A. S. Akingboye

Department of Earth Sciences, Adekunle Ajasin University, Akungba-Akoko, Nigeria

**ABSTRACT**

Igabi aerogravity dataset was interpreted to delineate litho-structural architectures that could favour the exploitation of potential economic minerals. The distribution of the gravity anomalies over the area ranged from –67.77 to –53.34 mGal. The upward continued bouguer anomaly maps at distance 500 m, 1 km, 2 km, 3 km, and 4 km revealed the variations of anomalous bodies with general regional trends in NW-SE, E-W, and NE-SW directions. The superimposed analytic signal indicated low amplitude signals for migmatites, schists, less dense felsic rocks (porphyritic granites) and fractures, while areas of high amplitude signals correlated with biotite granitic and gneissic rocks because of the denser mafic minerals in them. The second vertical derivative and tilt derivative maps revealed the anomaly patterns of shallow basement rocks and near circular closures anomalies that are associated with fractures within the granitic rocks. Spectral analysis suggested depth to gravity sources ranging between 0.3 km and 0.67 km for shallow, 0.90 km and 0.97 km for intermediate and 1.5 km to 1.86 km for deep sources, while Euler solution depths ranged from <1392.3 m to >2059 m. The results, therefore, suggested intense deformation of the basement rocks with tectonic framework suitable for mineralisation.

**ARTICLE HISTORY**
Received 13 May 2019
Revised 4 October 2019
Accepted 1 November 2019

**KEYWORDS**
Bouguer anomalies; litho-structures; spectral analysis; density; Igabi basement complex; Nigeria

## 1. Introduction

The dwindling crude oil economics in Nigeria offers the need for diversification of the nation's solid mineral base and resources. The economic potential and minable occurrence of uranium in Younger granite suite series of Igabi, Kajuru, Kachia and Kalatu sheets in Kaduna as well as Ririwai in northcentral Nigeria (Arisekola and Ajenipa 2013) necessitated the aero-gravity survey to unravel the conditions of the subsurface geological structures. The presence of significant anomalies of uranium mineralisation in Schist and Pan-African granitoids are also found in Kakuri and Bishini sheets in northwestern Nigeria (Arisekola and Ajenipa 2013).

Gravity method is a non-destructive geophysical method that measures the difference in the Earth's gravitational field at definite locations. Gravity surveys can be carried out on the earth's surface as ground gravity survey, in the air, which is known as "aero- or airborne-gravity survey", or at sea as "marine gravity survey". Gravity surveys are used for large-scale crustal study, where measurements of earth's gravitational field are used for mapping variations in subsurface rocks densities (Sultan et al. 2009; El-Bohoty et al., 2012; Mandal et al. 2013, 2015; Biswas et al. 2014a, 2014b), basement topography, sedimentary basin alongside its structural architecture, and for regional groundwater exploration. Other applications include environmental and engineering investigations, among others, Gravity interpretations are aimed at delineating the subsurface litho-structures and other features such as amplitude, shape, density contrast, frequency and closure of the gravity anomalies from bouguer anomaly, residual and regional maps/profiles and numerous enhancement maps.

Previous several studies have used second vertical derivative and 2D spectral analysis on bouguer data for delineation of lithological boundaries at Gusau area of Nigeria (Aku 2014). Ekpa et al. (2018) and Ofoha et al. (2018) investigated Niger Delta Basin of Nigeria through the interpretation of aero-gravity data to determine the thickness of the sediments, establish the basement topography, density contrasts and structural evaluation which will give information about variations in geological lithologies and structures. Other gravity enhancement techniques like Euler deconvolution and analytic signal map the trends of subsurface geologic lithologies and estimate of depths of structures based on the density contrast of the rocks. Therefore, this work is aimed at interpreting preliminary high-resolution gravity data through different enhancement techniques to delineate subsurface lithologies, structures and estimate the depth to top of gravity sources based on density contrasts of subsurface rocks in the study area.

**CONTACT** C. C. Okpoli cyril.okpoli@aaua.edu.ng Department of Earth Sciences, Adekunle Ajasin University, P.M.B. 001, Akungba-Akoko, Ondo State, Nigeria

## 2. Geologic setting of the study area

The study area (aero-gravity Sheet 124 NE covering Igabi area of Kaduna State, Northwestern Nigeria) lies between longitudes 007° 30′ and 008°00′E and latitudes 10°30′ and 11°00′N within the Precambrian Basement Complex of Northwestern Nigeria (Figure 1(a,b)). The area is about 30 km southwest of Zaria and has 253.57 km$^2$. The Precambrian rocks of Nigeria may be grouped into three principal subdivisions, which include Migmatite–Gneiss Complex (MGC), Schist belt (metasedimentary and metavolcanic rocks), Older granites (Pan-African granitoids) that also comprised the undeformed acid and basic dykes (Solomon 2010). The study area has been affected by two successive phases of intense deformation that resulted to tight isoclinal ENE to WSW and NS axes. These two progressive metamorphisms accompanied by deformation, were later separated and followed by static metamorphic phases. These areas are considered to be Upper Proterozoic supracrustal (schistose) rocks which have been in folded into the Migmatite-Gneiss-Quartzite complex (Rahaman 1988).

The Basement Complex rocks in the study area are grouped into two, namely: Migmatite-Gneiss Complex and the Pan-African granitoids. The Migmatite-Gneiss Complex is Neo-Proterozoic to Meso-Archaean (542Ma-3200Ma) in age and composed of migmatites and gneisses (Solomon 2010). It is the most extensive rock type in the area. The Pan-African granitoids are Pan-African (600 ± 200Ma) in age and consist mainly of granites, diorites and dolerites. Both the migmatites and gneisses were deformed and intruded by the Pan-African granitoids during the 600 ± 200 Ma Pan-African episodes. Figure 1(b) shows the lineaments/faults associated with these Precambrian Basement Complex rocks, with NE-SW and NW-SE trends (Rahaman et al. 1983).

The occurrence of uranium ores are found in the Younger granite series and uranium-rich granitoids around Igabi, Kajuru, kalatu and Kachia in Kaduna State as well as Naraguta and Maijuju sheet and in all associated Ririwai Ring Complex in northcentral and northwestern Nigeria (Arisekola and Ajenipa 2013). The region is also made up of highly fractured and poorly exposed weathered granite gneisses and fractured gneissic rocks. The granite gneiss belongs to the Pan-African Migmatite – Gneiss Complex, which forms part of the predominant rock units as observed in Figure 1(b). Minor lithological units include quartz veins and prominent veins in aplite dykes; these occur with structural features comprising joints, lineaments/faults and foliations (Solomon 2010).

## 3. Materials and methods of study

The purpose of gravity data study is to locate and describe subsurface structures from the observed

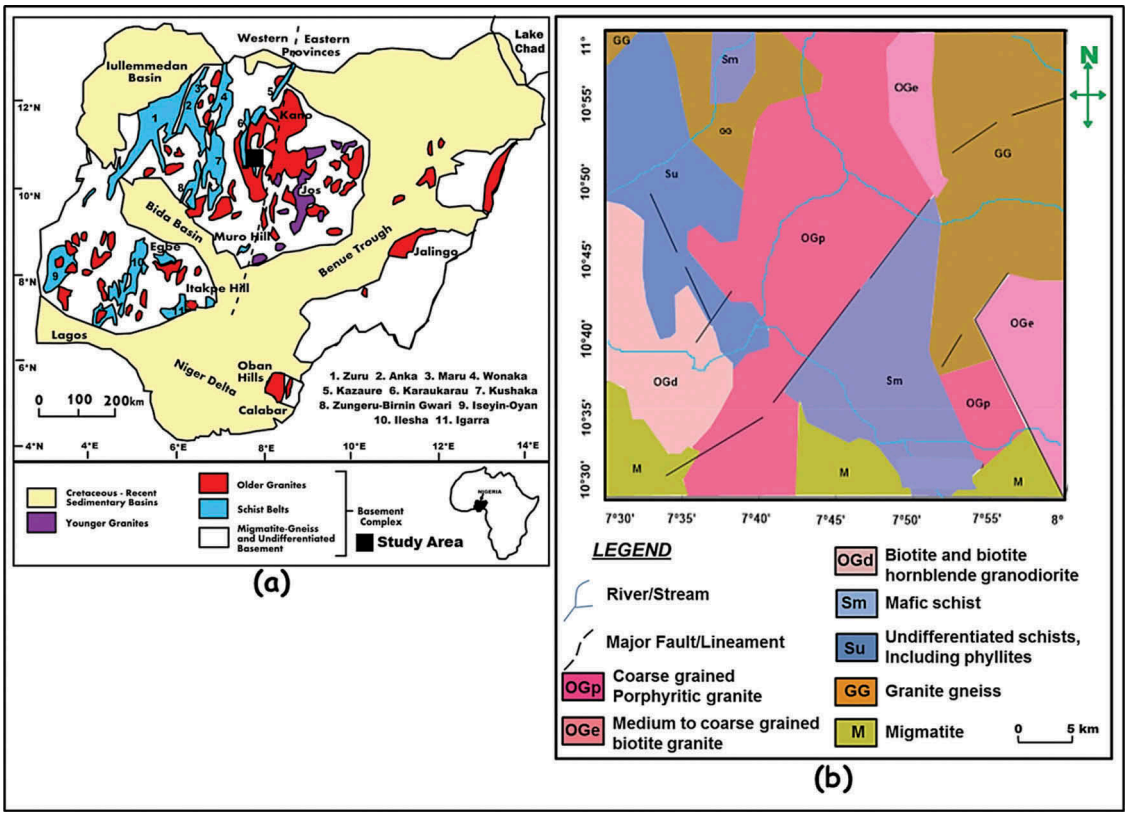


Figure 1. (a) Regional geological setting of Nigeria showing the study area (modified after Woakes et al. 1987) [Inset: Map of Africa showing Nigeria]. (b) Geological map of the study area (digitised from Geological Map of Nigeria 2004).

gravity effects caused by their anomalous densities (Telford et al. 1990; Lowrie 2007). The aero-gravity dataset used for this study was acquired from Nigerian Geological Survey Agency (NGSA) in Geosoft file format. The agency applied some sorts of reductions/corrections like drift correction, latitude, elevation, terrain/topography, free air, bouguer and Eotvos. The bouguer gravity dataset is of high resolution and the data were acquired at a terrain clearance of about 80 m height, flight line spacing of 500 m and tie-line spacing of 2 km in Northeast-Southwest direction. The modelling software used for data processing, analysis and interpretation of the bouguer dataset include Geosoft® Oasis Montaj™ software version 6.4.2 H.J and Surfer ™ version 12. The acquired bouguer dataset was gridded for the application of various forms of data reductions and enhancement in order to achieve the objectives of this study. The data reductions and enhancement techniques include residual field, upward continuation, analytic signal, second vertical derivative (2VD), tilt derivative (TDR), radially averaged power spectrum (RAPS) and Euler deconvolution.

The residual field which is the local field of interest arising from shorter-wavelength gravity anomalies was derived by removing the regional field caused by gentle trend long-wavelength gravity anomalies associated deep-seated basement features from the observed bouguer anomalies. The regional bouguer gravity field was produced by upward continuing the bouguer anomaly data to a depth of 4 km. The utilised upward continuation enhancement technique smoothens out shorter wavelength anomalies after the determination of the gravity field at an elevation higher than that at which the gravity field was measured (Hakim et al. 2006; Ganiyu et al. 2013). Upward continuation filter was used in smoothing and suppressing the effect of shallow anomalies, in order to acquire information on deeper anomalies. The most important effects of this filter on the data are basically to infer the effects of depth of continuation on gravity sources which are associated with the basement rocks and geological structures, as well as to reveal the regional basement anomaly trends.

The analytic signal method, also known as the total gradient method, produces a particular type of calculated gravity anomaly enhancement map used for defining the edges/boundaries of geologically anomalous density distributions (Hakim et al. 2006), and depth of the anomaly sources (Al-Badani and Al-Wathaf 2017). The use of analytic signal amplitude poses attractive features for any sort of potential field prospecting (Nabighian 1972, 1974). Its useful geophysical property is that it peaks exactly over the edge of the buried dipping contact that causes the anomalies. The 2VD technique is one of the several methods of removing regional trends. The technique sharpens the edges of anomalies which help to locate their positions. Some of the gravity anomalies are distinct on examination of bouguer map, but weak anomalies arising from shallower sources of limited depth and lateral extents are obscured by the presence of stronger gravity effects associated with deeper features of larger dimensions (Aku 2014). The applications of the 2VD in gravity interpretation to enhance localised small and weak near-surface features (i.e. improving the resolving power of the gravity map) have long been established (Baranov 1975; Gupta and Ramani 1982). The TDR filter attempts to place an anomaly directly over its source (Okpoli and Oladunjoye 2017; Akingboye et al. 2018). TDR assists in estimating contact locations of bodies at depth (Ndousa-Mbarga et al. 2012; Oyeniyi et al. 2016), and identifying areas of anomaly structures that are least affected by interference where repeated depth estimates are most likely to be reliable (Salem et al. 2007).

Power spectrum is a 2D function of energy and wave number and is generally used for identifying the average depth of source assemblages (Spector and Grant 1970). Spectral analytical tool is a well-established tool for estimating the depths of magnetised bodies (Bhattacharyya 1966; Mishra and Naidu 1974; Blakely 1996). Several authors, such as Spector and Grant (1970); Garcia and Ness (1994); Tatiana and Angelo (1998), explained the 2D spectral analysis technique. Keating (1995) applied 3-dimensional (3D) Euler deconvolution technique to airborne gravity and magnetic datasets while Zhang et al. (2000) also applied Euler deconvolution to gravity tensor gradient data. 3D Euler deconvolution has been further extended and generalised to cope with a wider range of source types (Mushayandebvu et al. 2001; Stavrev and Reid 2007, 2010; Reid et al. 2014). We also quantitatively interpreted the bouguer anomaly map to determine the depth to the top of gravity sources and trends and dimensions of anomalous sources. The adopted quantitative techniques include spectral analysis using RAPS and 3D Euler deconvolution techniques.

## 4. Discussion of results

The analysed bouguer anomaly map (Figure 2) from −67.77 to −53.34 mGal denoting variations in density properties of the rocks. According to Karner and Watts (1983), negative bouguer anomaly amplitude result is owed to the mountainous regions, where the survey was carried out; thereby reducing out the attraction of the mountainous mass. Very high negative gravity anomaly (−53.34 mGal) marked *A* seen as a circular closure in the southwestern part of the area indicates the presence of subsurface denser rocks. The northeastern and southeastern parts of the area marked *B* show areas with very low gravity anomalies

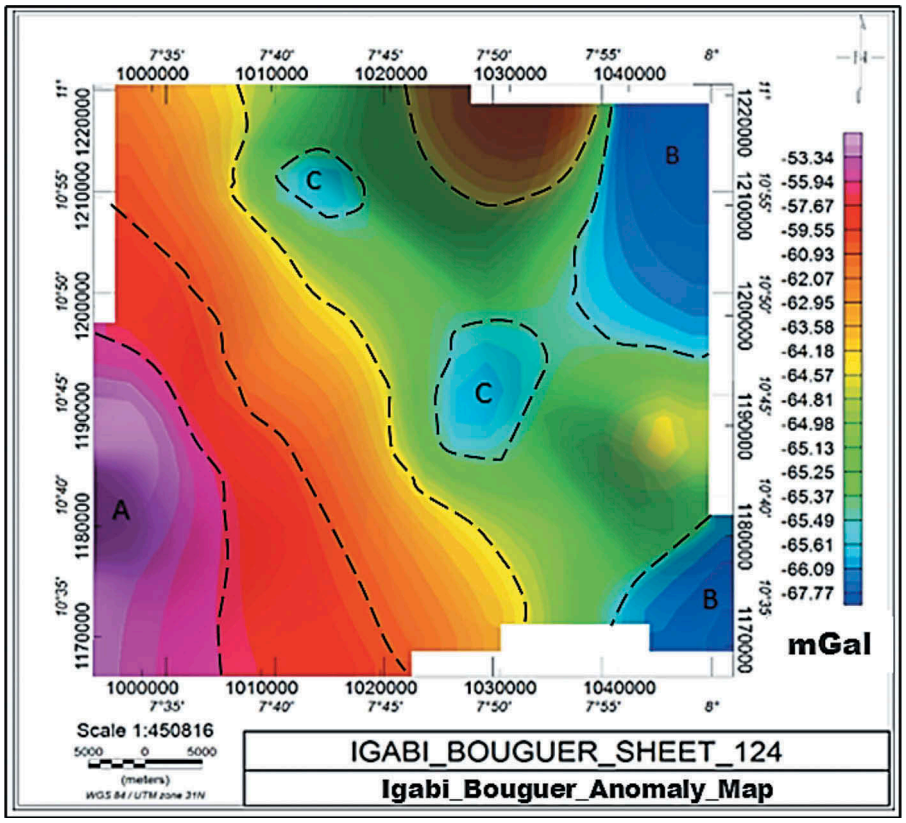


**Figure 2.** Bouguer anomaly map of the study area. Points A and B indicate area of very high and very low gravity anomalies, respectively, while points annotated as C are areas with intermediate gravity anomalies.

(< −66 mGal). These may be attributed to the presence of less dense and deformed rocks in the study area. At the central part of the northern axis of the area, sub-rounded shapes to approximately straight linear trends of NW-SE and NE-SW directions marked *C* with fairly low to moderately high gravity anomalies (−66 mGal to −64.5 mGal) are delineated. These observed features may suggest fractured zones, edges and contacts of different rocks in the area. Generally, most of the anomalies present in the area trend in NW-SE direction.

The residual gravity field reflects the distribution of lateral density variations within the crust and highlights concealed lithologies. Figure 3 displays maximum anomaly value of 1.60 mGal at the northern and southwestern parts and minimum anomaly value of less than −1.33 mGal at the southwestern and some parts of northeastern section of the study area. High gravity anomalies marked *A* at the southwestern, northeastern and western parts of the area may suggest the presence of subsurface shallower or near surface uplifted and denser basement rocks. Low to moderate gravity anomalies revealed at the northwestern and southwestern end, as well as the central to the northwestern end of the study area may possibly be less dense rocks, which may have been affected by intense metamorphism that produced the observed lineaments/faults in the area. The anomalies in the study area occur in different shapes and polarity with general trends/patterns in WNW-ESE, NW-SE and NE-SW directions.

The upward continuation method shows clearly the attenuation/reduction of short-wavelength anomalies with respect to the increase in observation to source distance. Figures 4(a–e) show the maps of the upward continued bouguer anomaly data to height of 500 m, 1 km, 2 km, and 3 km and 4 km, respectively. Generally, all the upward continuation maps reflect varying gravity anomalies with respect to height of upward continuation. High to very high gravity anomalies (> −64 mGal) occupy a portion of about half of the study area; occurring on the western parts with an approximate trend of NW-SE direction while very low to intermediate gravity anomalies (< −64 mGal) occupy the other half. However, high gravity anomalies with circular closures occur within low-density regions (Figure 4(a–c)). These observed circular closures anomalies reduced with upward continuation depth above 2 km and disappeared at depth of continuation above 3 km (Figure 4(d,e)). Areas occupied by high to very high gravity anomalies suggest subsurface denser rocks. On the other hand, intermediate gravity anomaly at the central part with similar trend of NW-SE, and very low to low anomalies

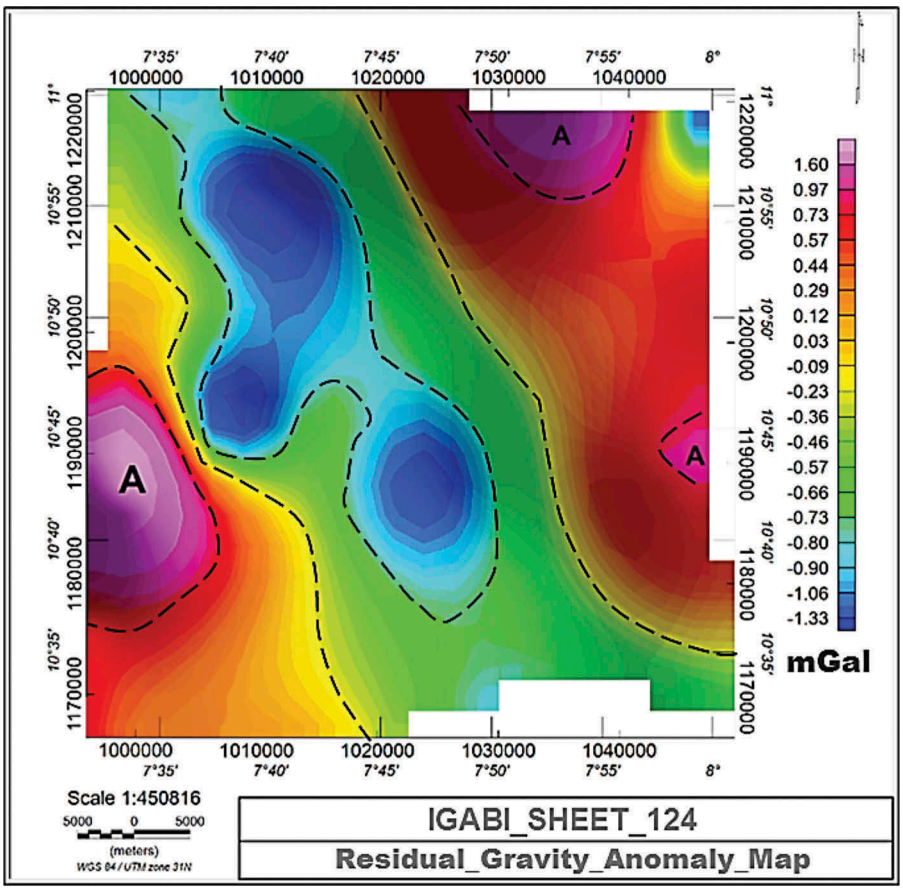


**Figure 3.** Residual bouguer anomaly map of the study area. Point A indicates areas with denser crustal rocks within the study area.

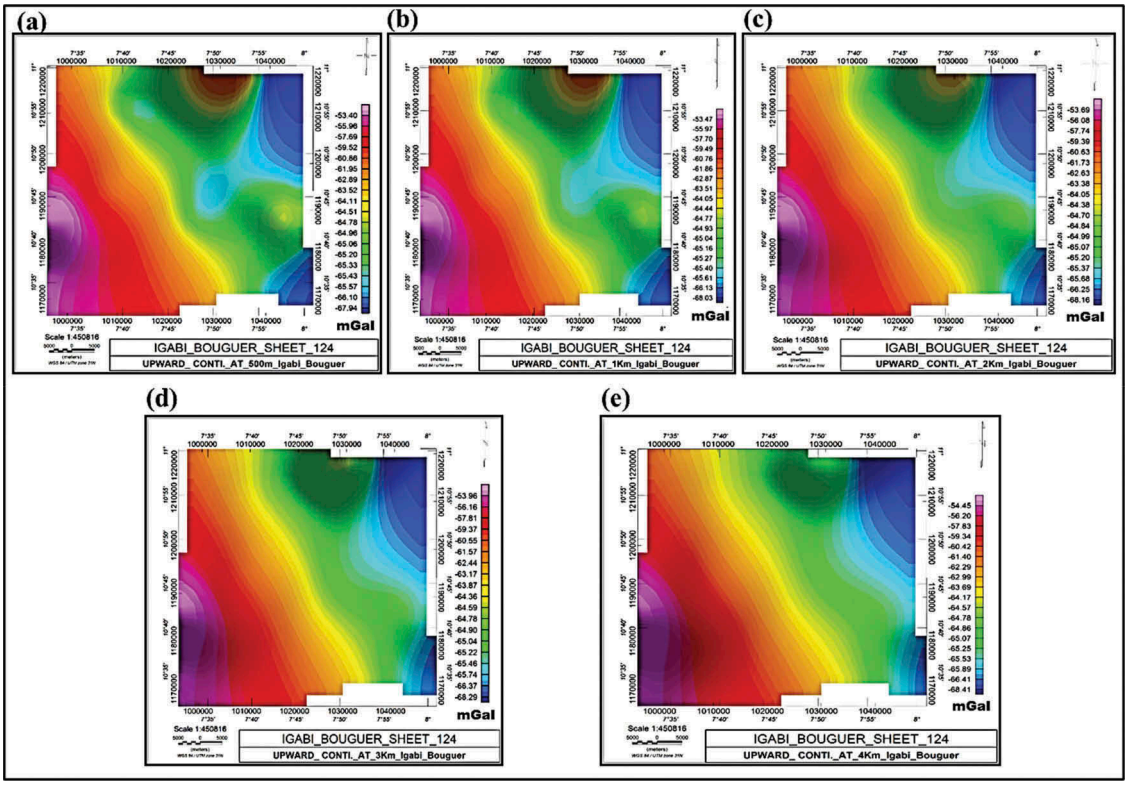


**Figure 4.** Upward continuation of Igabi bouguer anomaly to 500 m (a), 1 km (b), 2 km (c), 3 km (d) and, 4 km (e).

with trend of approximately NE-SW may be regarded as lineaments/faults that host viable economic minerals in the areas, such as uranium mineralisation in Pan African granitoid and mafic schist (Arisekola and Ajenipa 2013). Two of the very low bouguer anomalies width are elongated to circular gravity closures and closures increases with depth of continuations, but finally joined and changed trending direction to NW-SE at depth of upward continuation from 3 km and above (Figure 4(d,e)). The observed variations in widths and trends may have suggested shallow to intermediate depths with late of metamorphism for the delineated lineaments/faults with NE-SW, and deeper depths for those in NW-SE direction.

Figures 5(a,b) show the analytic signal gravity anomaly map and the superimposed map of the analytic signal gravity map on the geological map of the study area, respectively. The bouguer analytic signal map (Figure 5(a)) shows high amplitude signal values that ranged above 0.006 mGal/m at the western and northeastern parts denoted as P4 and P5, respectively. The areas with high analytic signals probably correspond to high-density contrasts generated by denser and shallower biotite granitic and gneissic rocks (Figure 5(b)). Points P1 and P2 are points of very low amplitude signal (0.0001–0.002) mGal/m with an NW-SE trend. These zones are suggested as highly fractured migmatites, schistose and less dense felsic rocks (porphyritic granites). The highlighted arrows on the map mark some of the edges/boundaries of rocks and the zones of weaknesses that are lineaments/faults are denoted as P1 and P2 in NW-SE direction with oblong curved shape low amplitude signal; these fractures are the most pronounced and deep penetrating fractures in the area. The other NE-SW trending lineaments/faults (P3 and P6) extend into and beyond the NW-SE trending structures, but they are at near surface depth than those earlier delineated. The superimposed map (Figure 5(b)) further confirms the litho-structural relationships that exist in the study area based on varying density contrasts revealed by various rocks. Figure 5(b) shows that most of the delineated subsurface lineaments/faults by the analytic signal enhancement technique agree with the directions of surface fractures on the geological map, but Figure 5(a) clearly shows the extension and trends of the mapped surface fractures deep in the subsurface.

Second vertical derivative (2VD) gravity anomaly map (Figure 6) reveals that some of the anomalies have been accentuated and re-positioned when compared to the bouguer anomaly map (Figure 2), though still evinced relatively similar features compared with the residual bouguer map (Figure 3). High gravity anomalies >0.0001 mGal/m occupy parts of the northern, eastern and the southwestern (marked as *A*) sections; indicating denser rock types than those in other sections of the map. Point *L* with intermediate gravity anomaly may probably be an alteration zone of shallower depth. Point *B* and *C* show areas of low to fairly low gravity anomaly which may be associated with fractured rocks in the area. This map reveals that the general trends of the shallower anomalous bodies are mainly NW-SE, NE-SW, and E-W (minor) directions.

The TDR map (Figure 7) delineates the anomalous conditions of the subsurface and are indicated by successive closed contours represented by high and low-frequency gravity anomalies on the map. The region enclosed by the 0° and distance between +45° and −45° (±1.5 radians) contours signifies the approximate location of the source edges and shallow basement rocks, respectively. The horizontal distance from the 45° to the 0° position is equivalent to the depth to top of the contact, or half distances between +45° and −45° (Al-Badani and Al-Wathaf 2017). The circular to oblong closures anomalies observed around the

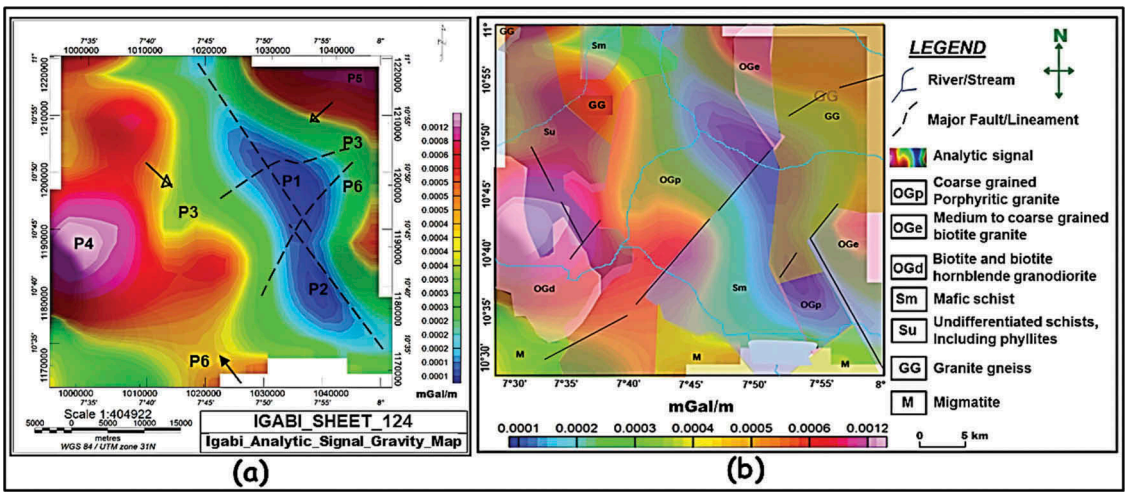


**Figure 5.** (a) Analytic signal gravity anomaly map. (b) Superimposed analytic signal gravity anomaly map on the geological map of the study area. P1 and P2 are points of very low amplitude signals, P3 and P6 are intermediate amplitude signal points while P4 and P5 are points of high amplitude signals.

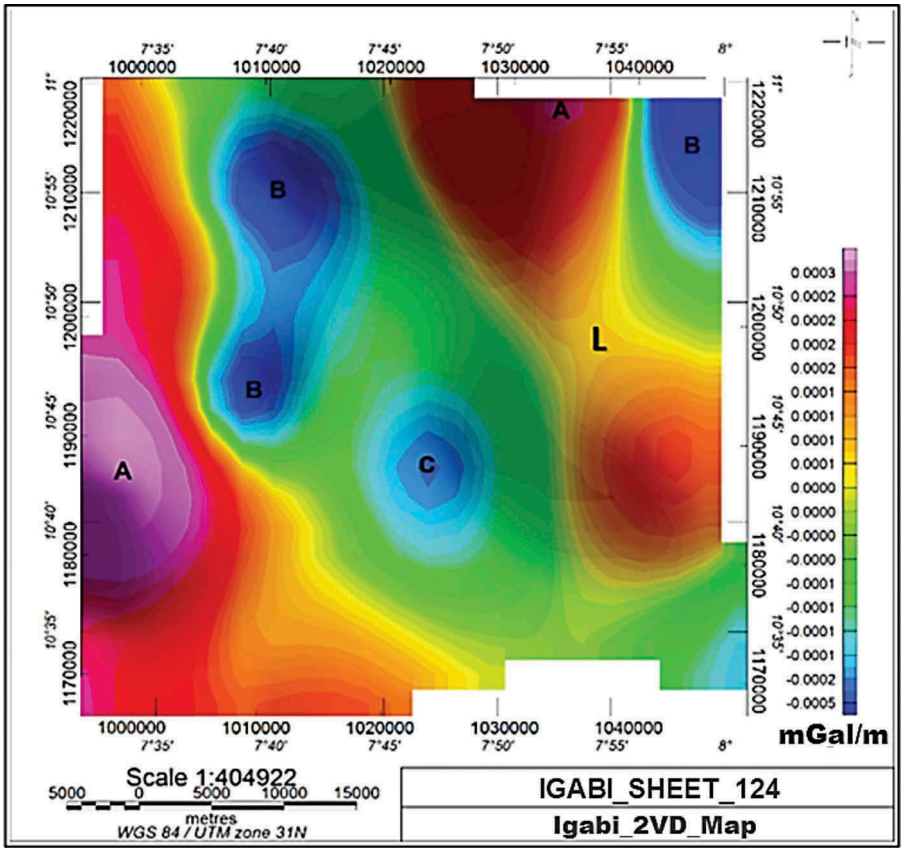


**Figure 6.** Second vertical derivative (2VD) anomaly map. Regions marked A and L indicate areas with very high and intermediate gravity anomalies, respectively, while points B and C indicate areas with very low to low gravity anomalies, respectively.

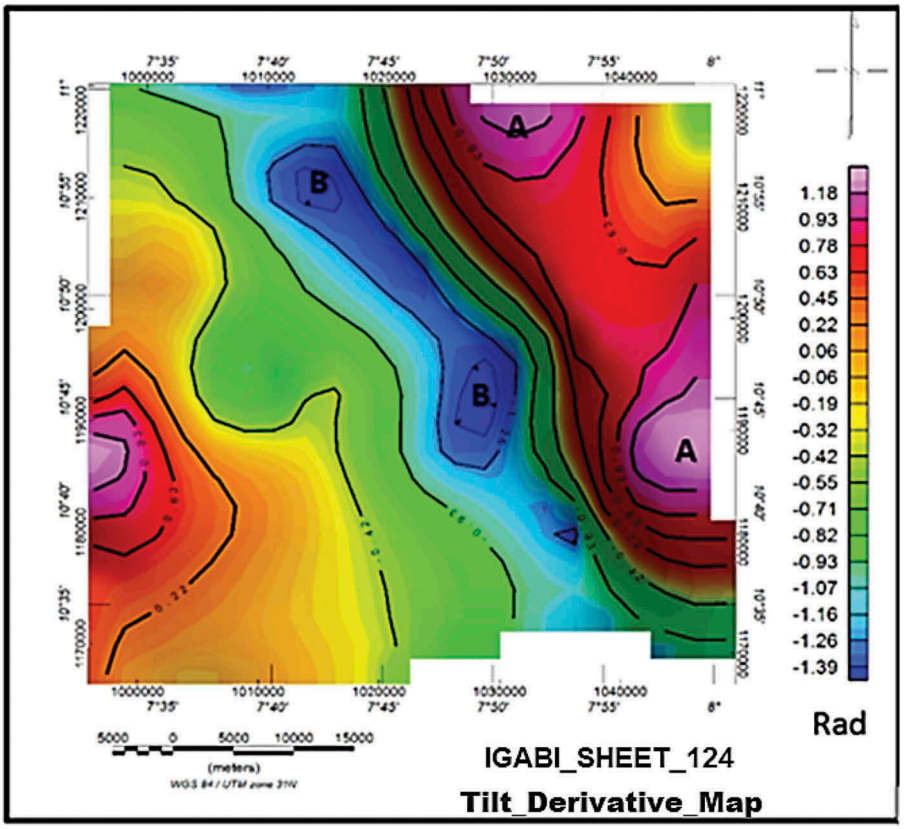


**Figure 7.** Contoured colour shaded tilt derivative bouguer map of the study area. Points A and B are points of high and low-frequency gravity closures, respectively.

central region of the western part of the bouguer map may be associated with granitic bodies in the area. Points denoted *A* are classified as areas of very high gravity anomaly probably due to its rock density. Points *B* mark the edges of the zone of weaknesses within the rocks of the area. The weak zones confined the edges and trends of the pronounced lineaments/faults mainly in NW-SE direction as seen at the central half of the map.

Figure 8 shows the radially averaged power spectrum (RAPS) or spectral analysis of the bouguer anomaly data. The bouguer anomaly map was divided into two spectral blocks to produce their radial spectrum and depth estimate maps (Figure 8(a,b)). Three depth sources which include shallower (blue line), intermediate (yellow line) and deeper sources (red line) were delineated on the 2D spectrum of respective spectral blocks based on wavelengths of density anomalous sources. The coordinates and various depths to top of density sources for respective quadrants are shown in Table 1. The shallower, intermediate, and deeper depths are 0.3 km, 0.9 km and 1.9 km and 0.2 km, 1.00 km, and 1.9 km for spectral block 1and 2, respectively. These estimated depths are only to the top of anomalous gravity sources in the area.

Euler deconvolution structural indices (S.I) of different source types, namely *S.I* 0.0, *S.I* 1.0, and *S.I* 2.0 were applied to the bouguer anomaly data used for this study. *S.I* 0.0 was used for delineating line cylinder, thin sheet edge, thin sill and dyke; *S.I* 1.0 for delineating line cylinder and thin line belt, and *S.I* 2.0 for delineating point and sphere (Reid et al. 2014). Euler deconvolution technique was not only used for delineating trends of subsurface structures, but also for determining the average depth of gravity sources (Sultan et al. 2017).

The structural solutions results (Figure 9(a–c)) are scanty, but still reveal the different structural index models: locations, edges and trends of different subsurface structures, as well as depths to the anomalous sources. *S.I* 0.0 solution result (Figure 9(a)) reveals some of the trends and edges (indicated by arrows) of the thin sheet and thin dykes/sills with the approximate trend of NW-SE and indication of tectono-metamorphic phases of Pan-African orogeny that harbour the uranium-rich granite mineralisation. *S.I* 1.0 solution result (Figure 9(b)) clearly reveals the line cylinders, and *S.I* 2.0 solution result (Figure 9(c)) on the other hand was able to show point and spherical structures in the study area. All the Euler deconvolution structural indices solutions showed that the lithological structures in the study area are mainly concentrated at central part while other parts like the western, northern and southern sections of this area have fewer structural features. These results further confirm that the central part and small parts of the western, northern and southern sections of the study area are characterised by highly deformed/fractured schistose rocks while the granitic rocks of the area are probably intrusive dykes. The obtained Euler anomalies depths ranged from <-1392.3 m to >2059 m over the mining zones suggesting that mineralisation around the study area is structurally controlled. The structural indices of pipes, ring-like and sphere models when applied were consistent with the delineated areas as observed from the contact/dyke models. The shortfall of a definite solution for a structural index of 2.0, diagnostic of pipe, sphere or ring-like massive anomalous body, might suggest that

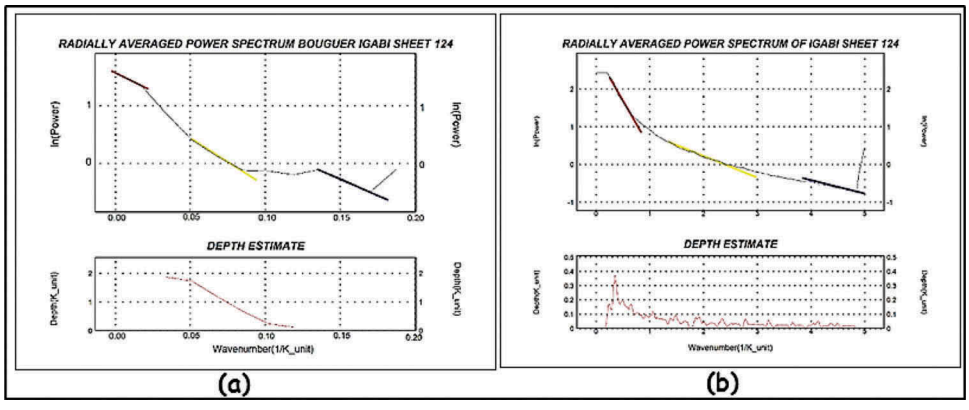


**Figure 8.** Spectral analysis of the Igabi gravity anomaly.

**Table 1.** Depth estimates to top of gravity sources derived from spectral analyses.

| | Easting (mE) | | Northing (mN) | | Depth (km) | | |
|---|---|---|---|---|---|---|---|
| Spectral block | $X_{min}$ | $X_{max}$ | $Y_{min}$ | $Y_{max}$ | Shallower | Intermediate | Deeper |
| 1 | 992293 | 1022518 | 1190546 | 1219530 | 0.30 | 0.90 | 1.90 |
| 2 | 1019247 | 1047104 | 1189530 | 1219869 | 0.20 | 1.00 | 1.90 |

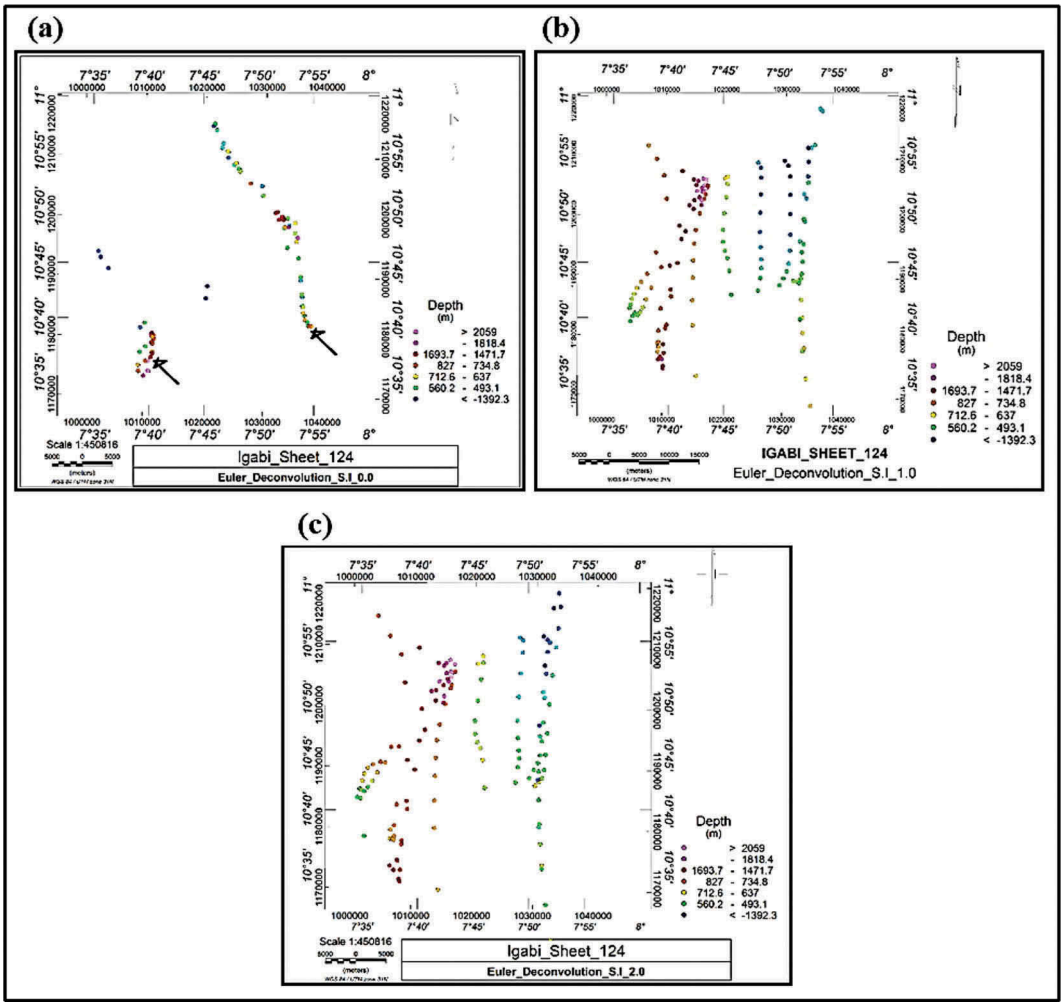


**Figure 9.** Euler deconvolution solutions of the Igabi gravity anomaly for S.I 0.0 (a), S.I 1.0 (b), and S.I 2.0 (c).

the mineralisation is disseminated as observed from the presence of low scale mining in the study area.

## 5. Conclusions

In this study, high-resolution gravity data analyses and enhancement techniques were carried out to reveal the locations, edges/boundaries, trends, and depths of litho-structures around Igabi area (Sheet 124 NE), Northwestern Nigeria. The analysed results of the bouguer anomaly and residual maps of Igabi show the distribution of the gravity anomalies and magnitudes of the concealed shear and weak zones being characterised by low to very high gravity anomalies. The upward continued bouguer anomaly maps at distance 500 m, 1 km, 2 km, 3 km, and 4 km reveal the variations of the deep-seated basement rocks, the structures and the mineralised anomalous bodies with depth. The upward continuation maps also show that the regional trends of the mapped lithologies and lineaments/faults in the area are generally in NW-SE, E-W, and NE-SW directions. Furthermore, the analytic signal gravity and its superimposed maps reveal areas with low to high amplitude signals. Low amplitude regions are probably dominated by migmatites, schistose, less dense felsic rocks (porphyritic granites) and fractures. On the other hand, high amplitude regions are likely occupied by denser biotite granitic and gneissic rocks. The maps also show some of the lineaments/faults in the area to be trending in NW-SE and NE-SW directions. In addition, the 2VD gravity anomaly map reveals that parts of the northern, eastern and the southwestern sections of the study area are characterised by denser basement rock than other parts particularly the central part of the study area.

TDR map shows circular to oblong closures anomalies observed around the central region which may be associated with fractures within the granitic bodies in the area. It also maps out the edges of the basement rocks and the intra-basement lineaments/faults with trend mainly in NW-SE direction. The spectral analysis of the RAPS results suggest depth to the top of gravity sources between 0.3 km and 0.67 km for shallow, 0.90 km to 0.97 km for intermediate and 1.5 km to 1.86 km for deep sources. Euler solutions show different subsurface structural features that include thin sheets and thin dykes/sills (with trend of NW-SE), line cylinder and sphere, as well as depth of basement rocks that range between less than

−1392.3 m to depth over 2054 m. The uranium mineralisation in the study area is believed to be hosted in the shallow zones being structurally controlled in NW-SE direction.

The generated maps can serve as spotlight for further exploration of mineralised zones in the study area which could be substantiated by core drilling. Aero radiometric survey, ground follow-up and geochemical surveys should be carried out in the study area to quantify the extent of other mineralisation and viable economic minerals hosted in the delineated mineralised zones.

## Acknowledgement

The authors deeply appreciate the reviews of the two anonymous reviewers for their insightful critiques that brought excellence in this manuscript.Many thanks to NGSA for the release of aerogravity dataset.

## Disclosure statement

No potential conflict of interest was reported by the authors.

## ORCID

C. C. Okpoli http://orcid.org/0000-0003-2844-3244

## References

Akingboye AS, Ademila O, Ogunyele AC. 2018. Improved magnetic data analyses and enhancement techniques for lithological and structural mapping around Akure, Southwestern Nigeria. Earth Scis Malaysia. 2(1):16–21.

Aku MO. 2014. Application of second vertical derivative analytical method to bouguer data for the purpose of delineation of lithological boundaries. Sci World J. 9(3):27–32.

Al-Badani MA, Al-Wathaf YM. 2017. Using the aeromagnetic data for mapping the basement depth and contact locations, at southern part of Tihamah region, western Yemen, Egypt. Egypt J Pet. doi:10.1016/j.ejpe.2017.07.015

Arisekola TM, Ajenipa RA 2013. Geophysical data results preliminary application to uranium and thorium exploration. IAEA-CYTED-UNECE workshop on UNFC-2009 at Santiago; 9-12, July, 12; Chile .

Baranov V. 1975. Potential fields and their transformations in applied geophysics. Explor Monogr Series. 65:58–69.

Bhattacharyya BK. 1966. Continuous spectrum of the total magnetic field anomaly due to a rectangle prismatic body. Geophysics. 31:97–121.

Biswas A, Mandal A, Sharma SP, Mohanty WK. 2014a. Delineation of subsurface structure using self-potential, gravity and resistivity surveys from South Purulia Shear Zone, India. Implication to Uranium Mineralization Interpretation. 2(2):103–110.

Biswas A, Mandal A, Sharma SP, Mohanty WK. 2014b. Integrating apparent conductance in resistivity sounding to constrain 2D Gravity modeling for subsurface structure associated with uranium mineralization across South Purulia Shear Zone. Int J Geo, vol. 2014, Article ID 691521: 1–8.

Blakely RJ. 1996. Potential Theory in Gravity and magnetic applications. U.K: Cambridge University Press.

Ekpa MM, Okeke M1, Ibuot FN, Obiora JC, Abangwu DN. 2018. Investigation of gravity anomalies in parts of Niger Delta Region in Nigeria using aerogravity data. Int J Phys Sci. 13(4):54–65. doi:10.5897/IJPS2017.4700.

El-Bohoty M, Brimich L, Saleh A, Saleh S. 2012. Comparative study between the structural and tectonic situation of southern Sinai, and red sea, Egypt, as deduced from magnetic, gravity, and seismic data. National Res Inst Astron Geophys. 42(2): 357–388.

Ganiyu SA, Badmus BS, Awoyemi MO, Akinyemi1 OD, Oluwaseun TO. 2013. Upward continuation and reduction to pole process on aeromagnetic data of Ibadan Area, South-Western Nigeria. Earth Sci Res. 2(1):66–73. doi:10.5539/esr.v2n1p66.

Garcia JG, Ness GE. 1994. Inversion of the power spectrum from magnetic anomalies. Geophysics. 59:391–400.

Geological Map of Nigeria. 2004. Nigerian Geological Survey AGENCY (NGSA), Garki. Abuja.

Gupta VK, Ramani N. 1982. Optimum second vertical derivatives in geologic mapping and mineral exploration. Geophysics. 47:1706–1715.

Hakim S, Jun N, Sachio E, Essam A. 2006. Integrated gradient interpretation techniques for 2D and 3D gravity data interpretation. Earth Planets Space. 58:815–821.

Karner GD, Watts AB. 1983. Gravity anomalies and flexure of the lithosphere at mountain ranges. J Geophys Res. 88 (B12):10.499–10.477.

Keating P. 1995. Error estimation and optimization of gravity surveys - Keating geophysical prospecting. 43(4): 569–580.

Lowrie W. 2007. Fundamentals of geophysics. London: Cambridge University Press.

Mandal A, Biswas A, Mittal S, Mohanty WK, Sharma SP, Sengupta D, Sen J, Bhatt AK. 2013. Geophysical anomalies associated with uranium mineralization from Beldih mine, South Purulia Shear Zone, India. J Geol Soc India. 82(6):601–606.

Mandal A, Mohanty WK, Sharma SP, Biswas A, Sen J, Bhatt AK. 2015. Geophysical signatures of uranium mineralization and its subsurface validation at Beldih, Purulia District, West Bengal, India: A case study. Geophys Prospect. 63:713–726.

Mishra DC, Naidu PS. 1974. Two dimensional power spectral analysis of aeromagnetic fields. Geophys Prospect. 22:345–534.

Mushayandebvu M, van Drielz P, Reid A, Fairhead J. 2001. Magnetic source parameters of two-dimensional structures using extended euler deconvolution. Geophysics. 66(3):814–823.

Nabighian MN. 1972. The analytic signal of two-dimensional magnetic bodies with the polygonal cross-section: its properties and use for automated anomaly interpretation. Geophysics. 3(37):507–517.

Nabighian MN. 1974. Additional comments on the analytic signal of two-dimensional magnetic bodies with polygonal cross section. Geophysics. 39:507–517.

Ndousa-Mbarga T, Fenmoue ANS, Manguelle-Dicoum E, Fairhead JD. 2012. Aeromagnetic data interpretation to locate buried faults in south-East Cameroon. Geophysica. 48(1–2):49–63.

Ofoha CC, Emujakporue G, Ekine AS. 2018. Structural evalution of bouguer gravity data covering parts of Southern Niger Delta, Nigeria. Arch Curr Res Int. 1–18 (3):1–18. doi:10.9734/ACRI/2018/40199.

Okpoli CC, Oladunjoye MA. 2017. Precambrian basement architecture and lineaments mapping of Ado-Ekiti region, using aeromagnetic dataset. Geosci Res. 2(1):27–45.

Oyeniyi TO, Salami AA, Ojo SB. 2016. Magnetic surveying as an aid to geological mapping: a case study from Obafemi Awolowo University campus in Ile-Ife, Southwestern Nigeria. Ife J Sci. 18(2):331–343.

Rahaman MA, 1988. Recent advances in the study of the basement complex of Nigeria. First Symposium on the Precambrian Geology of Nigeria proceedings, Kaduna, Special Publication of Geological survey of Nigeria.

Rahaman MA, Emofureta WO, Vachette M. 1983. The potassic-grades of the Igbeti area: further evaluation of the polycyclic evolution of the Pan African Belt in South-western Nigeria. Precambrian Resour. 22:75–92.

Reid AB, Jorg E, Webb SJ. 2014. Avoidable Euler Errors – the use and abuse of Euler deconvolution applied to potential fields. Geophysical prospecting. 1–7.

Salem A, Williams S, Fairhead J, Ravat D, Smith R. 2007. Tilt-depth method: a simple depth estimation method using first-order magnetic derivatives. Leading Edge. 26 (12):1502–1505.

Solomon AR 2010. Geology, geochemistry and genesis of Amethyst mineralization and association and associated rocks in Dutse Bakura Hill, Northcentral Nigeria. Unpublished MSc project submitted to Ahmadu Bello University, Zaria.

Spector A, Grant FS. 1970. Statistical models for interpreting aeromagnetic data. Geophysics. 35:293–302.

Stavrev P, Reid AB. 2007. Degrees of homogeneity of potential fields and structural indices of Euler deconvolution. Geophysics. 71:1–12.

Stavrev P, Reid AB. 2010. Euler deconvolution of gravity anomalies from thick contact/fault structures with extended negative structural index. Geophysics. 75:151–158.

Sultan SA, Mekhemer HM, Santos FA, Abd Alla M. 2009. Geophysical measurements for subsurface mapping and groundwater exploration at the central part of the Sinai Peninsula, Egypt. The Arabian J Sci Eng. 34(1A):17.

Sultan SA, Mohamed E, Abou HM, Mahmoud EI, Ahmed K, Enas M, Abd E. 2017. Implementation of magnetic and gravity methods to delineate the subsurface structural features of the basement complex in central Sinai area, Egypt. NRIAG J Astron Geophys. 1–28. doi:10.1016/j.nrjag.2017.12.002

Tatiana FQ, Angelo S. 1998. Exploration of a lignite bearing in Northern Ireland, using Maurizio ground magnetic. Geophysics. 62(4):1143–1150.

Telford WM, Geldart LP, Sheriff RE, Keys DA. 1990. Applied Geophysics. 2nd ed. Cambridge University Press; p. 744.

Woakes M, Rahaman MA, Ajibade AC. 1987. Some metallogenetic features of the Nigerian basement. J Afr Earth Sci. 6(5):655–664. doi:10.1016/0899-5362(87)90004-2.

Zhang C, Mushayandebvu MF, Reid AB, Fairhead JD, Odegard ME. 2000. Euler deconvolution of gravity tensor gradient data. Geophysics. 65:512–520.